Voronoi Diagrams Bordering the Escape Regions
for the Target-Attacker-Defender Problem

Mostafa Ali Rushdi, Ayman H. Kassem, Gamal El-Bayoumi

Department of Aerospace Engineering
Cairo University
Cairo, Egypt
morushdi@gmail.com, draymank@yahoo.com, gelbayoumi@yahoo.com

Abstract

This paper deals with an important pursuit-evasion problem that involves three agents, the Target the Attacker and the Defender. The Attacker missile pursues a Target aircraft that is being helped by a Defender missile which tries to intercept the Attacker before it reaches the Target. A differential game arises in which a team is formed by the Target and the Defender which cooperate to maximize the separation between the Target and the point where the Defender intercepts the Attacker, while the Attacker tries to minimize this separation. This paper offers a unified analytic treatment of the aforementioned problem based on the construction of two Apollonius circles. The treatment includes all possibilities of the ratio between the speeds of the Attacker and Defender. A criticality condition is derived from which two important entities are obtained, namely: (a) the critical Target speed normalized wrt the Attacker's speed, and (b) the Voronoi diagram bordering the safe or escape region for the Target. Beside unifying previously published results in a common setting, this paper simplifies all computations by using intuitionistic plane-geometric arguments rather than the more tedious analytic-geometric manipulations. Moreover, the paper extends existing results by adding some novel results, thereby giving a complete picture of all cases of interest. The analysis in this paper is supplemented by extensive computations using MATLAB to plot the Voronoi diagrams under a variety of pertinent parameters. The numerical results and plots obtained allow useful and insightful interpretation.

Keywords: Pursuit-Evasion, Target, Attacker, Defender, Apollonius circle, critical speed ratio, Escape region, Voronoi diagram.

1. Introduction

This paper deals with a scenario of active target defence involving three-agent pursuit-evasion where each agent has a specific role. A two-agent team consists of a Target (aircraft) and a Defender (missile) cooperating in opposition to an Attacker (missile). The Target tries to evade the Attacker and avoid being captured by him. The Defender cooperates with and assists the Target by trying to intercept(capture and destroy) the Attacker before the latter captures the Target [1, 2, 3, 4, 5, 6]. This problem will be referred to herein as the TAD problem as it concerns a triad consisting of the Target(T), Attacker(A), and Defender(D).

The TAD problem constitutes a dynamic differential game [7, 8, 9, 10, 11, 12, 13, 14, 15] and is of interest in aerospace, control, and robotics engineering. We will consider herein recent formulation and treatments of this problem [1, 2, 3, 4, 5, 6], though there exist other formulations and treatments of it that span almost half a century [16, 17, 18, 19, 20, 21, 22, 23, 24, 25]. Table 1 shows several variants of this generic problem in a variety of settings, contexts or disciplines. The TAD problem is a generalization of the classical problem of a single pursuer and a single evader [26, 27, 28, 29, 30]. In fact, the TAD is essentially a duplication of this classical problem, since in the TAD problem, the Attacker plays the double role of being a pursuer for the Target, and at the same time an evader for the Defender [19]. The TAD problem is also a special case of a more general pursuit-evasion problem in which there are multiple Attackers and multiple Defenders [31, 32, 33, 34, 35]. Many common threads are shared by all these problems, such as the solution of differential games [7, 8, 9, 10, 11, 12, 13, 14, 15] and the construction of Apollonius circles [36, 37, 38, 39] and Voroni diagrams [40, 41, 42, 43, 44, 45, 46, 45].

This paper offers a unified analytic treatment of the aforementioned TAD problem based on the construction of two Apollonius circles. The treatment includes all possibilities of the ratio between the speeds of the Attacker and Defender. Note that the case of a slow Defender appears here for the first time, while the treatment of the cases of fast Defender or similar Defender is extended and augmented with novel results and new insights. A criticality condition is derived from which the two following important entities are obtained

- the critical Target speed normalized w.r.t. the Attacker's speed so as to be a dimensionless quantity,

- the Voronoi diagram bordering the safe or escape region for the Target.

Beside unifying previously published results in a common setting, this paper simplifies all computations by using in-

Table 1: A variety of settings or contexts for the same generic problem

Area	Agent 1	Agent 2	Agent 3	References
Aerospace	Target	Attacker(missile)	Defender(missiles)	[1, 2, 3, 4, 5]
Biology	Prey	Predator	Protector	[20, 25]
Society	Lady	Bandits	Bodyguards	[18]
Criminology	Robber	Policemen/Cops	Gangsters	[42]

tuitionistic plane-geometric arguments rather than the more tedious analytic-geometric manipulations. Moreover, the paper extends existing results by adding some novel results, thereby giving a complete picture of all cases of interest. The analysis in this paper is supplemented by extensive computations using MATLAB to solve the complex high-order polynomial equations and to plot the Voronoi diagrams under a variety of pertinent parameters. The numerical results and plots obtained allow useful and insightful interpretations.

The organization of the remainder of this paper is as follows. Section II lists the assumptions, notation and nomenclature used herein. Section III discusses the general concepts and properties of an Apollonius circle [36, 37, 38, 39], and then specializes these to the cases of the AD Apollonius circle and the TA Apollonius circle. Section IV derives a criticality condition which constitutes a quadratic equation that is later solved for the critical dimensionless ratio between the Target speed and Attacker speed. The same criticality condition is then rephrased in Section V as a relation between the initial coordinates x_T and y_T of the Target. This relation leads to the Voronoi diagram bordering the *safe* or *escape* region R_e of the Target. This Voronoi diagram is published for the first time when the Defender is fast or slow. It includes as a special case the much simpler diagram for a similar Defender that has already appeared in [3]. Section VI concludes the paper and points out possible directions for further work.

2. ASSUMPTIONS, NOTATION, AND NOMENCLA-TURE

2.1. ASSUMPTIONS

1. The speeds V_T, V_A, and V_D of the Target, Attacker, and Defender are constant.
2. The Attacker missile is faster than the Target aircraft, i.e., $\alpha \equiv \dfrac{V_T}{V_A} < 1$ (In the case $\alpha \geq 1$, the Target is guaranteed to survive by following an optimal strategy, even without assistance from the Defender).
3. There are three distinct cases for the ratio of the speed of the Attacker to that of the Defender $\gamma = \dfrac{1}{\beta} = \dfrac{V_A}{V_D}$
   - $\gamma < 1$ (fast Defender) discussed earlier in Garcia et el. [2], and extended, expounded, simplified and exposed herein.
   - $\gamma = 1$ (same speed Defender) discussed in Garcia et el. [1, 3], and extended, expounded, simplified and exposed herein.

- $\gamma > 1$ (slow Defender), which is a novel case, discussed herein for the first time, and unified with the two previous cases.
4. The Defender intercepts the Attacker if their separation becomes zero (point capture).
5. The optimal trajectories of the three agents are straight lines.
6. A Cartesian frame is attached to the initial positions A and D of the Attacker and Defender in such a way the X-axis is the infinite extension of the straight segment $\overline{AD}$ and the Y-axis is the perpendicular bisector of $\overline{AD}$.

2.2. NOTATION
- A: Initial position of the Attacker.
- D: Initial position of the Defender.
- T: Initial position of the Target.
- T' Terminal position of the Target, i.e., its position at the time the Defender intercepts the Attacker.
- $\alpha = \dfrac{V_T}{V_A}$ (assumed < 1, otherwise the target trivially survives).
- $\gamma = \dfrac{1}{\beta} = \dfrac{V_A}{V_D}$ (studied for a fast Defender ($\gamma < 1$), a similar Defender ($\gamma = 1$), and a slow Defender ($\gamma > 1$)).
- u, v, w: Aim points on the AD Apollonius circle by the Attacker, Target and Defender, respectively.

2.3. NOMENCLATURE
2.3.1. The AD Apollonius circle
The locus of a point such that the ratio of its distance from the initial positions $A = (x_A, 0)$ and $D = (-x_A, 0)$ of the Attacker and Defender, respectively, is a fixed ratio $\gamma = \dfrac{V_A}{V_D}$. This circle degenerates into the perpendicular bisector of $\overline{AD}$ if $\gamma = 1$. Points on the circumference of this circle are reached simultaneously by the Attacker and Defender. For $\gamma < 1$, A belongs to the interior of this circle and points within the circle are reached by the Attacker before the Defender. For $\gamma > 1$, D belongs to the interior of this circle and points within the circle are reached by the Defender before the Attacker. For $\gamma = 1$, the AD circle becomes of infinite radius and degenerates into a straight line, namely the perpendicular bisector of $\overline{AD}$. In this case, A belongs to the R.H.S. of the XY−plane where points are reached by the Attacker before the Defender, while D belongs to the L.H.S. of the XY−plane where points are reached by the Defender before the Attacker.

2

2.3.2. The TA Apollonius circle

The locus of a point such that the ratio of its distances from the initial positions $T = (x_T, y_T)$ and $A = (x_A, 0)$, of the Target and Attacker, respectively, is a fixed ratio $\alpha = \dfrac{V_T}{V_A}$ strictly less than 1. Naming of the AD and TA Apollonius circles herein follows a common practice in mathematical circles [36, 37, 38] and is opposite to the style used by Garcia et al. [1, 2, 3].

2.3.3. Region reachable by the Defender before the Attacker (Reachability region R_r)

For $\gamma < 1$, R_r is the exterior of the AD Apollonius circle.
For $\gamma = 1$, R_r is the L.H.S. of the $XY-$plane.
For $\gamma > 1$, R_r is the interior of the AD Apollonius circle.

Figure 1 illustrates this region as a shaded region to which point D belongs.

2.3.4. Region of guaranteed Target's escape (Escape region R_e)

The escape region R_e is the set of all coordinate pairs (x, y) such that if the Target initial position $T = (x_T, y_T)$ is inside this region, then it is guaranteed to escape the Attacker if both the Target and Defender implement their corresponding optimal strategies. This set is a strict superset of the set of points reachable by the Defender before the Attacker ($R_e \supseteq R_r$). The boundary of this set is called a Voronoi Diagram.

2.3.5. The critical speed ratio $\bar{\alpha}$

A lower limit on the speed ratio $\gamma = \dfrac{V_T}{V_A}$, attained when the TA Apollonius circle is tangent to the AD Apollonius circle (or to the perpendicular bisector of $\overline{AD}$ in the degenerate case $\gamma = 1$).

2.3.6. Escape Condition

For a given speed ratio $\alpha = \dfrac{V_T}{V_A}$ and a given Attacker's initial position $A = (x_A, 0)$, the escape condition is that the TA Apollonius circle (of center O_2 and radius r_2) intersects the AD Apollonius circle (of center O_1 and radius r_1). This happens for $\gamma < 1$ when

$$|\boldsymbol{O_1} - \boldsymbol{O_2}| + r_2 > r_1 \tag{1}$$

It happens for $\gamma > 1$ when

$$|\boldsymbol{O_1} - \boldsymbol{O_2}| - r_2 < r_1 \tag{2}$$

In the degenerate case of $\gamma = 1$, it is required that the TA Apollonius circle intersects the $Y-$axis, i.e.,

$$r_2 > the\ abscissa\ of\ \boldsymbol{O_2} \tag{3}$$

3. APOLLONIUS CIRCLES PERTAINING TO THE *TAD* PROBLEM

A circle is the locus moving at a constant distance (called the circle's radius r) from a fixed point (called the circle's centre O). In the limit of an infinite radius ($r \longrightarrow \infty$), the circle degenerates into a straight line. Another definition of the circle

is that it is the locus of a point moving such that the ratio of its distances from two fixed points A and B is a constant k. With this definition, the circle is called a circle of Apollonius (in honour of Apollonius of Perga (ca. 262-190 BC), the Great Geometer of Antiquity). In the limit ($k \longrightarrow 1$) this circle degenerates into the perpendicular bisector of $\overline{AD}$, while in the two limits ($k \longrightarrow 0$) and ($k \longrightarrow \infty$), this circle collapses to the two points A and B, respectively.

Two Apollonius circles are studied herein, namely the AD Apollonius circle, and the TA Apollonius circle. The study will be based on simple and intuitive plane-geometric arguments and will avoid the more involved treatment of analytic geometry. Figures 2 and 3 shows the Apollonius circles for a moving point P such that $\dfrac{AP}{PB} = k \neq 1$. The case $k > 1$ is shown in Fig. 2, while the case $k < 1$ is shwon in Fig. 3. The points I and E are the two special cases of P that lie on the straight line extension of the straight segment $\overline{AB}$. These points divide the straight segment $\overline{AB}$ internally and externally in the ratio k ($k \neq 1$), i.e.,

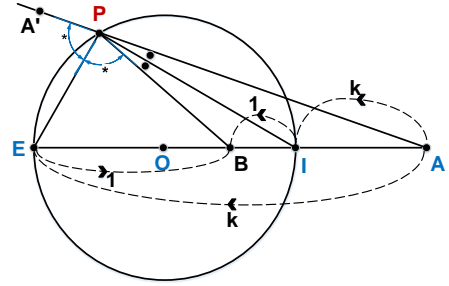$$\boxed{\frac{AI}{IB} = \frac{AE}{EB} = k, \ \{k \neq 1\}.} \tag{4}$$

Figure 2: Apollonius circle for a moving point P such that $\dfrac{AP}{PB} = k > 1$. Here $m\angle API = m\angle BPI$ and $m\angle A'PE = m\angle BPE$.
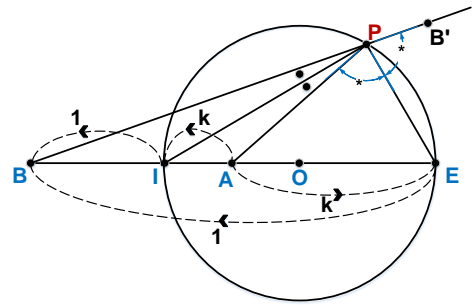
Figure 3: Apollonius circle for a moving point P such that $\dfrac{AP}{PB} = k < 1$. Here $m\angle API = m\angle BPI$ and $m\angle APE = m\angle B'PE$.

If we denote the position vector of a point by a bold version of its name, we can rewrite (4) in vectorial form as

$$(\boldsymbol{I} - \boldsymbol{A}) = k(\boldsymbol{B} - \boldsymbol{I}), \tag{5}$$

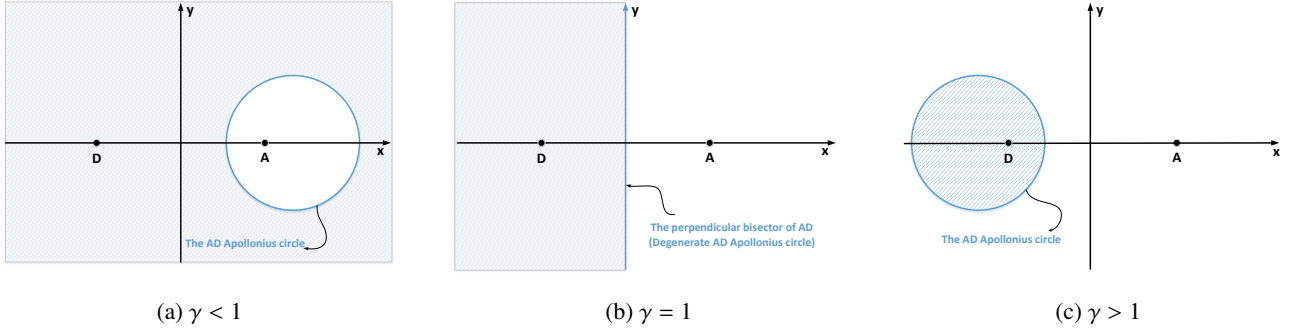(a) $\gamma < 1$ (b) $\gamma = 1$ (c) $\gamma > 1$

Figure 1: The reachability region R_r (one including D whose points are reached by the Defender before the Attacker) is shown shaded.

$$(E - A) = k(E - B), \tag{6}$$

which can be used to express I and E in terms of A and B as

$$I = \frac{1}{k+1}(A + kB), \tag{7}$$

$$E = \frac{1}{k-1}(-A + kB). \tag{8}$$

The Apollonius circle is easily characterized by the points I and E, since they are the two end points of one of the its diameters. The center of the circle is the midpoint of points I and E, namely:

$$\begin{aligned}
O &= \frac{1}{2}(I + E) \\
&= \frac{1}{2}[(\frac{1}{k+1} - \frac{1}{k-1})]A + k(\frac{1}{k+1} + \frac{1}{k-1})B \\
&= -\frac{1}{k^2-1}A + \frac{k^2}{k^2-1}B,
\end{aligned} \tag{9}$$

while the radius of the circle is half the length of the displacement from I to E,

$$\begin{aligned}
r &= \frac{1}{2}|I - E| \\
&= \frac{1}{2}|(\frac{1}{k+1} + \frac{1}{k-1})A + k(\frac{1}{k+1} - \frac{1}{k-1})B| \\
&= |\frac{k}{k^2-1}A - \frac{k}{k^2-1}B| \\
&= |\frac{k}{k^2-1}||A - B| = \frac{k}{k^2-1}(AB).
\end{aligned} \tag{10}$$

It is clear from (9) and (10) that $\lim_{k\to 1}|O| \to \infty$ and $\lim_{k\to 1} r \to \infty$, and hence for $k = 1$, the Apollonius circle degenerates into a straight line, namely the perpendicular bisector of the straight segment $\overline{AB}$ (Fig. 4).

3.1. The AD Apollonius circle

For the AD Apollonius circle, the two fixed points are the initial positions of the Attacker $A = (x_A, 0)$ and the initial position of the defender $D = (-x_A, 0)$. The fixed ratio of the circle
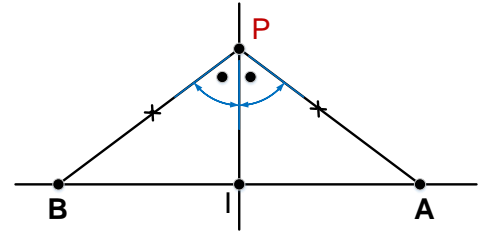

Figure 4: For $k = 1$, the Apollonius circle in figures 2 or 3 degenerates into the perpendicular bisector of the straight segment $\overline{AB}$. The point E disappears in this figure as it goes to ∞

k is replaced by the following dimensionless ratio which is the Attacker's speed normalized w.r.t the Defender speed:

$$\gamma = \frac{V_A}{V_D}. \tag{11}$$

We will consider the three cases of

1. $\gamma < 1$ (fast Defender) discussed in Garcia et al. [2].
2. $\gamma = 1$ (same-speed Defender) discussed in Garcia et al. [1, 3].
3. $\gamma > 1$ (slow Defender), which is a novel case.

Substituting the values of A and D above for A and B in (7),(8),(9) and (10), respectively, and replacing k therein by γ we obtain for $\gamma \neq 1$,

$$I_1 = (\frac{1-\gamma}{1+\gamma}x_A, 0), \tag{12}$$

$$E_1 = (\frac{1+\gamma}{1-\gamma}x_A, 0), \tag{13}$$

$$O_1 = (\frac{1+\gamma^2}{1-\gamma^2}x_A, 0), \tag{14}$$

$$r_1 = \frac{2\gamma}{|1-\gamma^2|}x_A. \tag{15}$$

Three interesting sets of limits are now considered. The first set of limits are those when ($\gamma \to 1$), namely

4

$$\lim_{\gamma \to 1} \boldsymbol{I}_1 = (0,0), \tag{16}$$

$$\lim_{\gamma \to 1} \boldsymbol{E}_1 = (\mp\infty, 0), \tag{17}$$

$$\lim_{\gamma \to 1} \boldsymbol{O}_1 = (\mp\infty, 0), \tag{18}$$

$$\lim_{\gamma \to 1} r_1 = \infty, \tag{19}$$

which means that the *AD* Apollonius circle degenerates in the limit ($\gamma \to 1$) to a circle of an infinite radius with center still on the x−axis but infinitely distant from the origin. More precisely, this limit is identified as a straight line, namely the perpendicular bisector of the straight-line segment $\overline{AD}$.

The second set of limits are those when ($\gamma \to 0$), namely

$$\lim_{\gamma \to 0} \boldsymbol{I}_1 = (x_A, 0), \tag{20}$$

$$\lim_{\gamma \to 0} \boldsymbol{E}_1 = (x_A, 0), \tag{21}$$

$$\lim_{\gamma \to 0} \boldsymbol{O}_1 = (x_A, 0), \tag{22}$$

$$\lim_{\gamma \to 0} r_1 = 0, \tag{23}$$

which means that the *AD* Apollonius circle collapses in the limit ($\gamma \to 0$) to a single point, namely the initial position of the Attacker $\boldsymbol{A} = (x_A, 0)$.

The third set of limits are those when ($\gamma \to \infty$), namely

$$\lim_{\gamma \to \infty} \boldsymbol{I}_1 = (-x_A, 0), \tag{24}$$

$$\lim_{\gamma \to \infty} \boldsymbol{E}_1 = (-x_A, 0), \tag{25}$$

$$\lim_{\gamma \to \infty} \boldsymbol{O}_1 = (-x_A, 0), \tag{26}$$

$$\lim_{\gamma \to \infty} r_1 = 0, \tag{27}$$

which means that the *AD* Apollonius circle collapses in the limit ($\gamma \to \infty$) to a single point, namely the initial position of the Defender $\boldsymbol{D} = (-x_A, 0)$.

3.2. The TA Apollonius circle

For the *TA* Apollonius circle, the two fixed points are the initial position of the Target $\boldsymbol{T} = (x_T, y_T)$ and the initial position of the Attacker $\boldsymbol{A} = (x_A, 0)$. Again, the fixed ratio of the circle k is replaced by a dimensionless quantity, namely the Target's speed normalized w.r.t. the Attacker's speed:

$$\alpha = \frac{V_T}{V_A}. \tag{28}$$

Here, we will consider only the case $\alpha < 1$, since for $\alpha \geqslant 1$, the Target always survives, even without any assistance from the Defender.

Now, we substitute the values of $\boldsymbol{T}$ and $\boldsymbol{A}$ above for $\boldsymbol{A}$ and $\boldsymbol{B}$ in (7),(8),(9) and (10), respectively, and replace k therein by α to obtain:

$$\boldsymbol{I}_2 = \frac{1}{1+\alpha}(\boldsymbol{T} + \alpha\boldsymbol{A}) = \frac{1}{1+\alpha}(x_T + \alpha x_A, y_T), \tag{29}$$

$$\boldsymbol{E}_2 = \frac{1}{\alpha - 1}(-\boldsymbol{T} + \alpha\boldsymbol{A}) = \frac{1}{1-\alpha}(x_T - \alpha x_A, y_T), \tag{30}$$

$$\boldsymbol{O}_2 = \frac{1}{1-\alpha^2}(\boldsymbol{T} - \alpha^2\boldsymbol{A}) = \frac{1}{1-\alpha^2}(x_T - \alpha^2 x_A, y_T), \tag{31}$$

$$r_2 = \frac{\alpha}{1-\alpha^2}(TA) = \frac{\alpha d}{1-\alpha^2}, \tag{32}$$

where $d = TA =$ the initial distance between the target and Attacker, namely

$$d = \sqrt{(x_T - x_A)^2 + y_T^2}. \tag{33}$$

4. CRITICAL SPEED RATIO

Target survival is guaranteed if there is an overlapping of the region reachable by the Target before the Attacker (the interior of the TA Apollonius circle) and the region R_r reachable by the Defender before the Attacker (Fig. 1), since within this overlapping, the Defender can perform its intended role of intercepting the Attacker before the Attacker captures the Target. Target survival is critical when the aforementioned overlapping diminishes into a single point at which the aforementioned two regions barely touch, or are tangent to one another. For this situation, the normalized Target speed (the speed ratio) $\alpha = \dfrac{V_T}{V_A}$ attains its minimal or critical value $\overline{\alpha}$. Now, we consider three cases, in which the TA-Apollonius circle is tangent from outside to the boundary of the shaded region R_r. An implicit assumption throughout the forthcoming analysis is that $\boldsymbol{T} = (x_T, Y_T)$ is outside R_r.

4.1. The case $\gamma < 1$ (fast defender)

The critical speed ratio $\overline{\alpha}$, occurs when the TA Apollonius circle is *internally* tangent to the *AD* Apollonius circle, i.e., when the centers $\boldsymbol{O}_2$ and $\boldsymbol{O}_1$ of these two circles and their tangency point $\boldsymbol{C}$ are collinear (Fig. 5a). This happens when

$$r_1 - r_2 = |\boldsymbol{O}_1 - \boldsymbol{O}_2|. \tag{34}$$

Substituting for $r_1, r_2, \boldsymbol{O}_1$ and $\boldsymbol{O}_2$ from (15), (32), (15) and (31) respectively, and noting that $\gamma < 1$, one obtains

$$\frac{2\gamma}{1-\gamma^2}x_A - \frac{\alpha}{1-\alpha^2}d$$
$$= |(\frac{1+\gamma^2}{1-\gamma^2}x_A, 0) - \frac{1}{1-\alpha^2}(x_T - \alpha^2 x_A, y_T)| \tag{35}$$
$$= [(\frac{1+\gamma^2}{1-\gamma^2}x_A - \frac{1}{1-\alpha^2}(x_T - \alpha^2 x_A))^2 + \frac{1}{(1-\alpha^2)^2}y_T^2]^{\frac{1}{2}}.$$

In (35), we deliberately replaced $|1 - \gamma^2|$ by $(1 - \gamma^2)$ because $\gamma < 1$. We now square both sides of (35) to obtain:

$$\frac{4\gamma^2}{(1-\gamma^2)^2}x_A^2 + \frac{\alpha^2}{(1-\alpha^2)^2}d^2 - \frac{4\gamma\alpha d}{(1-\gamma^2)(1-\alpha^2)}x_A =$$

$$= \frac{(1+\gamma^2)^2}{(1-\gamma^2)^2}x_A^2 + \frac{x_T^2 - 2\alpha^2 x_T x_A + \alpha^4 x_A^2}{(1-\alpha^2)^2} \qquad (36)$$

$$-\frac{2(1+\gamma^2)(x_T - \alpha^2 x_A)x_A}{(1-\gamma^2)(1-\alpha^2)} + \frac{1}{(1-\alpha^2)^2}y_T^2.$$

By squaring both sides of equation (35), the cardinality of the solution set for equation (35) is doubled. This means that when we solve the resulting equation, half of the resulting solutions will be extraneous or irrelevant and have to be rejected. Fortunately, we will have genuine reasons that enable us to identify such solutions, and compel us to reject them. The solutions retained after such a rejection are the correct solutions of (34) We now use (33) to replace y_T^2 by $(d^2 - x_A^2 - x_T^2 - 2x_A x_T)$ and rearrange terms in (36) to obtain

$$[\frac{4\gamma^2}{(1-\gamma^2)^2} - \frac{(1+\gamma^2)^2}{(1-\gamma^2)^2} - \frac{\alpha^4}{(1-\alpha^2)^2} - \frac{2\alpha^2(1+\gamma^2)}{(1-\gamma^2)(1-\alpha^2)} + \frac{1}{(1-\alpha^2)^2}]x_A^2$$

$$+[\frac{\alpha^2}{(1-\alpha^2)^2} - \frac{1}{(1-\alpha^2)^2}]d^2$$

$$-\frac{4\gamma\alpha x_A d}{(1-\gamma^2)(1-\alpha^2)} + [\frac{-1}{(1-\alpha^2)^2} + \frac{1}{(1-\alpha^2)^2}]x_T^2$$

$$+[\frac{2\alpha^2}{(1-\alpha^2)^2} + \frac{2(1+\gamma^2)}{(1-\gamma^2)(1-\alpha^2)} - \frac{2}{(1-\alpha^2)^2}]x_T x_A = 0 \qquad (37)$$

The coefficient of x_A^2 in (37) is

$$\frac{4\gamma^2}{(1-\gamma^2)^2} - \frac{(1+\gamma^2)^2}{(1-\gamma^2)^2} - \frac{\alpha^4}{(1-\alpha^2)^2} - \frac{2\alpha^2(1+\gamma^2)}{(1-\gamma^2)(1-\alpha^2)} + \frac{1}{(1-\alpha^2)^2}$$

$$= \frac{4\gamma^2 - 1 - \gamma^4 - 2\gamma^2}{(1-\gamma^2)^2} + \frac{(1-\alpha^4)}{(1-\alpha^2)^2} - \frac{2\alpha^2(1-\gamma^2)}{(1-\gamma^2)(1-\alpha^2)}$$

$$= -1 + \frac{1+\alpha^2}{(1-\alpha^2)} - \frac{2\alpha^2(1+\gamma^2)}{(1-\gamma^2)(1-\alpha^2)}$$

$$= \frac{2\alpha^2}{(1-\alpha^2)} - \frac{2\alpha^2(1+\gamma^2)}{(1-\gamma^2)(1-\alpha^2)}$$

$$= \frac{2\alpha^2}{(1-\alpha^2)}[1 - \frac{(1+\gamma^2)}{(1-\gamma^2)}] = \frac{2\alpha^2}{(1-\alpha^2)}(\frac{-2\gamma^2}{(1-\gamma^2)})$$

$$= \frac{-4\alpha^2\gamma^2}{(1-\alpha^2)(1-\gamma^2)}, \qquad (38)$$

and the coefficient of d^2 in (37) is

$$\frac{\alpha^2}{(1-\alpha^2)^2} - \frac{1}{(1-\alpha^2)^2} = \frac{-(1-\alpha^2)}{(1-\alpha^2)^2} = -\frac{1}{(1-\alpha^2)}, \qquad (39)$$

while the coefficient of $x_T x_A$ in (37) is

$$\frac{2\alpha^2}{(1-\alpha^2)^2} + \frac{2(1+\gamma^2)}{(1-\gamma^2)(1-\alpha^2)} - \frac{2}{(1-\alpha^2)^2}$$

$$= \frac{2(\alpha^2-1)}{(1-\alpha^2)^2} + \frac{2(1+\gamma^2)}{(1-\gamma^2)(1-\alpha^2)}$$

$$= -\frac{2}{(1-\alpha^2)} + \frac{2(1+\gamma^2)}{(1-\gamma^2)(1-\alpha^2)} \qquad (40)$$

$$= \frac{2}{(1-\alpha^2)}[-1 + (\frac{1+\gamma^2}{1-\gamma^2})] = \frac{2}{(1-\alpha^2)}(\frac{2\gamma^2}{1-\gamma^2})$$

$$= \frac{4\gamma^2}{(1-\alpha^2)(1-\gamma^2)}$$

This means that equation (37) can be simplified considerably to the equivalent form

$$\frac{-4\alpha^2\gamma^2}{(1-\alpha^2)(1-\gamma^2)}x_A^2 - \frac{1}{1-\alpha^2}d^2$$

$$-\frac{4\gamma\alpha x_A d}{(1-\gamma^2)(1-\alpha^2)} + \frac{4\gamma^2}{(1-\alpha^2)(1-\gamma^2)}x_T x_A = 0 \qquad (41)$$

Now, we multiply (41) by $[-(1-\alpha^2)(1-\gamma^2)]$ noting that $\alpha \neq 1$ and $\gamma \neq 1$, to obtain

$$(4\gamma^2 x_A^2)\alpha^2 + (4\gamma x_A d)\alpha + (1-\gamma^2)d^2 - 4\gamma^2 x_T x_A = 0 \qquad (42)$$

or equivalently

$$\boxed{\alpha^2 + \frac{d}{\gamma x_A}\alpha + [(\frac{1-\gamma^2}{4\gamma^2})(\frac{d}{x_A})^2 - \frac{x_T}{x_A}] = 0} \qquad (43)$$

Equation (43) is an improvement of equation (36) in [3]. while (43) is a quadratic equation in α, equation (36) in [3] is a quartic in α that has the same two roots of (43) in addition to the two irrelevant roots $\alpha \mp 1$. As a bonus, equation (43) is written in a self-verifying dimensionless form.

4.2. The case $\gamma = 1$ (similar Defender)

The critical speed ratio $\overline{\alpha}$ occurs when the TA Apollonius circle touches the $L.H.S.$ of the XY−plane (Fig. 5b), i.e., when

$$r_2 = Absicessa\ of\ \boldsymbol{O_2}. \qquad (44)$$

i.e., thanks to (31) and (32) when:

$$\frac{\alpha d}{1-\alpha^2} = \frac{x_T - \alpha^2 x_A}{1-\alpha^2}. \qquad (45)$$

Multiplying (45) by $(1-\alpha^2)$ (thanks to the fact that $\alpha \neq 1$), and rearranging, one obtains the following quadratic equation in α

$$x_A\alpha^2 + d\alpha - x_T = 0, \qquad (46)$$

which is equation (12) in [3]. It is interesting to note that equation (45) is the special case ($\gamma = 1$) of (43), though (43) was derived under the assumption $\gamma \neq 1$.

4.3. The case $\gamma > 1$ (Slow Defender)

The critical speed ratio $\overline{\alpha}$ occurs when the TA Apollonius circle is *externally* tangent to the AD Apollonius circle, i.e., when the centre $\boldsymbol{O_2}$, the tangency point $\boldsymbol{C}$ and the centre $\boldsymbol{O_1}$ are collinear(Fig. 5c), i.e., when

$$r_1 + r_2 = |\boldsymbol{O_1} - \boldsymbol{O_2}| \qquad (47)$$

Since $\gamma > 1$, we write

$$r_1 + r_2 = \frac{2\gamma}{|1 - \gamma^2|} + \frac{\alpha}{1 - \alpha^2}d = \frac{-2\gamma}{1 - \gamma^2} + \frac{\alpha}{1 - \alpha^2}d. \qquad (48)$$

The above expression for $(r_1 + r_2)$ is exactly the negative of $(r_1 - r_2)$ in (35). Hence, squaring of (47) results in (36), and consequently lead to (37) and (41), and finally to (42) and (43). Equation (43) is thereby shown to hold for a slow Defender besides being true for a fast one.

Therefore, we will use the quadratic formula (43) for all values of γ, and will solve it to obtain $\overline{\alpha}$ for any γ as

$$\begin{aligned}
\overline{\alpha} &= \frac{1}{2}[-\frac{d}{\gamma x_A} \pm [(\frac{d}{\gamma x_A})^2 - 4(\frac{1 - \gamma^2}{4\gamma^2})(\frac{d}{x_A})^2 + \frac{4x_T}{x_A}]^{1/2}] \\
&= \frac{1}{2\gamma x_A}[-d \mp \gamma\sqrt{d^2 + 4x_T x_A}] \\
&= \frac{1}{2\gamma x_A}[-\sqrt{(x_A - x_T)^2 + y^2} + \gamma\sqrt{(x_A + x_T)^2 + y_T^2}]
\end{aligned} \qquad (49)$$

Equation (49) was derived in [3] for $\gamma < 1$ and in [1] for $\gamma = 1$, provided $x_T > 0$. It is shown herein to hold for all values in γ, including $\gamma > 1$. Note that $\overline{\alpha}$ is definitely nonnegative and hence the minus sign in the solution for $\overline{\alpha}$ is rejected. The question remains whether (49) yields a non-negative value for $\overline{\alpha}$ when the positive sign is chosen in (49). It could be argued that (49) should be used (with the positive sign, of course) as long as it yields a nonnegative value for $\overline{\alpha}$, and otherwise $\overline{\alpha}$ should be set to zero. For example, if $\gamma = 1$ and $x_T < 0$, equation (49) yields a negative value for $\overline{\alpha}$ which need to be rejected and replaced by zero. Physically, the situation $\gamma = 1, x_T < 0$ is one in which the Target is initially in the region reachable by the Defender before the Attacker, i.e., it is within the effective protection of the Defender, even if it does not move itself at all. Therefor, we rewrite (49) in the following dimensionless form:

$$\overline{\alpha} = \frac{1}{2\gamma}[-\sqrt{(1 - \frac{x_T}{x_A})^2 + (\frac{y_T}{x_A})^2} + \gamma\sqrt{(1 + \frac{x_T}{x_A})^2 + (\frac{y_T}{x_A})^2}] \qquad (50)$$

provided that

$$\gamma\sqrt{(1 + \frac{x_T}{x_A})^2 + (\frac{y_T}{x_A})^2} > \sqrt{(1 - \frac{x_T}{x_A})^2 + (\frac{y_T}{x_A})^2} \qquad (51)$$

and whenever (51) is not valid, we simply set

$$\overline{\alpha} = 0. \qquad (52)$$

5. ESCAPE REGION AND VORONOI DIAGRAM

In this chapter, we develop a novel analytic expression for the pursuit-evasion Voronoi diagram [1] that marks or borders the "safe" or "escape" region R_e for the Target, i.e., the region defined by the set of all coordinate points (x, y) such that if the target's initial position (x_T, y_T) is inside this region, then the target is guaranteed to survive (to escape the Attacker) provided both the Target and Defender implement their optimal strategies, and regardless of the policy adopted by the Attacker, whether optimal or not. The Voronoi diagram obtain divides the XY−plane, into two regions

- a safe or escape region R_e to which the Defender's initial position $\boldsymbol{D}$ belongs.

- a *potentially* unsafe region to which the Attacker's initial position $\boldsymbol{A}$ belongs.

Garcia et al. [1] treated this problem for $\gamma = 1$ only using some involved arguments with inequalities developed from scratch, and without due reference to their earlier analysis concerning the critical speed ratio.

A very important *insight* that markedly simplifies our work is to note that required Voronoi diagram is simply a rephrasing of the criticality equation (43) for any value of γ including the cases $\gamma > 1$ or $\gamma < 1$ and $\gamma = 1$, viewed as a relation between y_T and x_T rather than a polynomial in α. Working with equalities is definitely simpler than working with inequalities, and it specifies a Voronoi diagram that divides the whole plane into two distinct parts, namely: the safe region and the (potentially) unsafe region. The safe region is then identified simply as the region to which $\boldsymbol{D}$ belongs. Note that the set of points of the safe regions R_e is a superset of the points reachable by the Defender before the Attacker R_r, i.e., $R_e \supseteq R_r$. The two regions R_e and R_r are identical if the Target does not move at all ($\alpha = 0$), a situation in which the Target does not exert any own effort to secure its survival and relies solely on the Defender's helping efforts. The family of Voronoi diagrams for various values of the normalized speed α will be bounded by the one for $\alpha = 0$, which is the border of R_r (Fig. 1).

Now, we obtain the general Voronoi diagram by rewriting the critically equation (43) or (42) as a relation between y_T and x_T. This is achieved via (33) to substitute $(x_A^2 + x_T^2 - 2x_A x_T + y_T^2)$ for d^2. To avoid mistakes in the manipulations, one must make sure that the pertinent equation at every step is dimensionally homogeneous. From (42), we write

$$(4\gamma\alpha x_A)d = -(1 - \gamma^2)d^2 + 4\gamma^2 x_A x_T - 4\gamma^2\alpha^2 x_A^2 \qquad (53)$$

Now, we square both sides of (53) to obtain

$$\begin{aligned}
&16\gamma^2\alpha^2 x_A^2(x_A^2 + x_T^2 - 2x_A x_T + y_T^2) \\
&= [-(1 - \gamma^2)(x_A^2 + x_T^2 - 2x_A x_T + y_T^2) + 4\gamma^2 x_A x_T - 4\gamma^2\alpha^2 x_A^2]^2 \\
&= [-(1 - \gamma^2)(x_A^2 + x_T^2 + y_T^2) + 2(1 + \gamma^2)x_A x_T - 4\gamma^2\alpha^2 x_A^2]^2
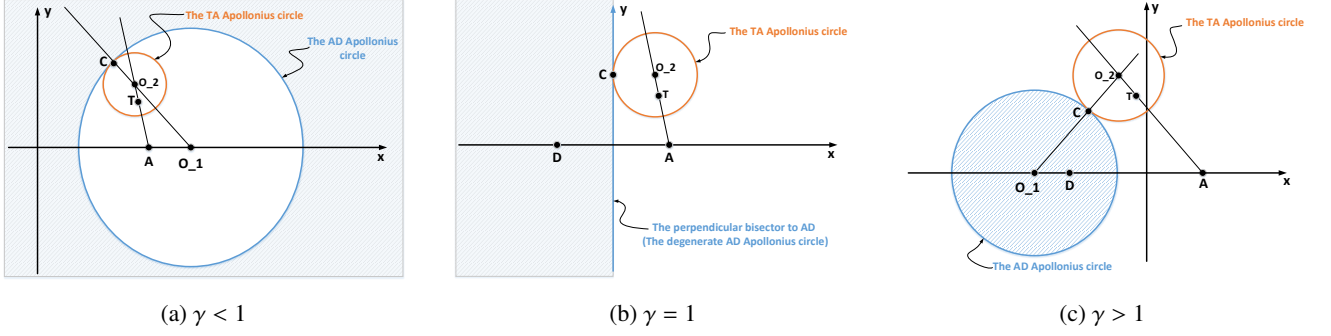\end{aligned}$$
$$(54)$$

(a) $\gamma < 1$ (b) $\gamma = 1$ (c) $\gamma > 1$

Figure 5: The critical speed ratio $\overline{\alpha}$ is obtained when the TA Apollonius circle is tangent to the boundary of the shaded region R_r which is the region reachable by the Defender befor the Attacker.

Now we rearrange (54) as a quartic equation (forth-degree polynomial) in x_T and y_T, namely

$$
\begin{aligned}
p(x_T, y_T) = {}& 16\gamma^2\alpha^2 x_A^4 \\
& + 16\gamma^2\alpha^2 x_A^2 x_T^2 \\
& - 32\gamma^2\alpha^2 x_A^3 x_T \\
& + 16\gamma^2\alpha^2 x_A^2 y_T^2 \\
& - (1-\gamma^2)^2[x_A^4 + x_T^4 + y_T^4 + 2x_A^2 x_T^2 + 2x_A^2 y_T^2 + 2x_T^2 y_T^2] \\
& - (1+\gamma^2)^2 * 4x_A^2 x_T^2 \\
& - 16\gamma^4\alpha^4 x_A^4 \\
& + 2(1-\gamma^4)(2x_A^3 x_T + 2x_A x_T^3 + 2x_A x_T y_T^2) \\
& - 8\gamma^2(1-\gamma^2)\alpha^2(x_A^4 + x_A^2 x_T^2 + x_A^2 y_T^2) \\
& + 16\gamma^2(1+\gamma^2)\alpha^2 x_A^3 x_T
\end{aligned}
\tag{55}
$$

Equation (55) is satisfied by the required Voronoi diagram. The quartic polynomial $p(x_t, y_T)$ satisfies

$$
p(x_T, -y_T) = p(x_T, y_T), \tag{56}
$$

since it has even powers only for y_T. This means $p(x_T, y_T)$ is an even function in y_T and its graph in the $x_T - y_T$ plane is *symmetric* w.r.t. the x_T-axis.

Though (55) is a quartic equation, the actual Voronoi diagram is expected to be a quadratic curve and not a quartic curve. Note that we performed a squaring operation in obtaining (42) and hence for obtaining (55), which doubled the pertinent degree from two to four. Hence, the Voronoi diagram is just a second-degree factor, part or branch of the fourth-degree curve depicted by (55). We will be able to identify the correct Voronoi diagram by rejecting any part of the curve that lies in R_r, i.e., the correct Voronoi diagram should define the border of R_e such that $R_e \supseteq R_r$.

Note that (55) is the general equation for the Voronoi diagram in our current TAD problem and it appears here for the first time. As a check on its correctness, we use it to produce the correct curve for $\gamma = 1$, earlier obtained by Garcia et al. [3], namely

$$
16x_A^2[-(1-\alpha^2)x_T^2 + \alpha^2 y_T^2] = -16x_A^4\alpha^2(1-\alpha^2), \tag{57}
$$

or equivalently

$$
\frac{x_T^2}{\alpha^2 x_A^2} - \frac{y_T^2}{(1-\alpha^2)x_A^2} = 1. \tag{58}
$$

Equation (57) represents a hyperbola which is an open curve of two branches. Interestingly enough the term hyperbola is believed to have been coined by our old friend Apollonius of Perga in his work on conic sections. This hyperbola is represented in Fig. 6 and has the following properties:

- The hyperbola has two focal points $F_1 = (c, 0)$ and $F_2 = (-c, 0)$, where

$$
c^2 = \alpha^2 x_A^2 + (1-\alpha^2)x_A^2 = x_A^2, \tag{59}
$$

  i.e. the focal points coincide with the initial positions of the Attacker $A = (x_A, 0)$ and the Defender $D = (-x_A, 0)$. Note that these two focal points are shared by an infinite set of curves for various values of α ($0 < \alpha < 1$).

- The line joining the focal points, i.e., the *transverse axis* coincides with the x_T-axis. The midpoint of the two focal points, i.e., the *center* of the hyperbola, is the origin $(0,0)$. The conjugate axis (the line perpendicular to the hyperbola's transverse axis through its center) is the y_T-axis.

- The eccentricity of the hyperbola e is

$$
e = \frac{c}{\alpha x_A} = \frac{1}{\alpha} > 1, \tag{60}
$$

  where the fact that $e > 1$ distinguishes the hyperbola from other conic sections, namely the ellipse (of $e < 1$) and the parabola (of $e = 1$). Note that the eccentricity e equals the ratio of the distance PF_i from a point P on the hyperbola to one focus F_i to the distance of the point to the corresponding directrix PQ_i, i.e.

$$
PF_i = e\, PQ_i, \quad i = 1, 2, \tag{61}
$$

- The vertices of the hyperbola (its intersections with the x_T-axis) are at $(\alpha x_A, 0)$ and $(-\alpha x_A, 0)$, and hence approach the two focal points as α tends to 1 (from below).

- Perpendicular to the transverse axis are the two directrices D_1 and D_2 given by

$$x_T = \mp\frac{\alpha x_A}{e} = \mp\alpha^2 x_A \qquad (62)$$

These directrices also approach the focal points when $\alpha \to 1$.

- The hyperbola has two asymptotes that intersect at its center, and are given by

$$y_T = \mp(\frac{\sqrt{1-\alpha^2}}{\alpha})x_T. \qquad (63)$$

For $0 < \alpha < 1$, the magnitude of the slope for an asymptote increases as α decreases and vice verse. Unlike the vertices and directrices, the asymptotes are independent of x_A.

- As a special case of the polynomial $p(x_T, y_T)$, in (55) the hyperbola (58) is an even function of y_T and hence is symmetric about the x_T-axis, Incidently the hyperbola is also even in x_T and hence its two branches are symmetric about the y_T-axis but this observation is irrelevant since only one branch is retained in further study.

- In the limit ($\alpha \to 0$), the hyperbola (58) degenerates into the y_T-axis.

- In the limit ($\alpha \to 1$), the right branch or the hyperbole (58) degenerates into a ray emanating from A in the positive direction of the x_T-axis, while its left branch degenerates into a ray emanating from D in the opposite direction.
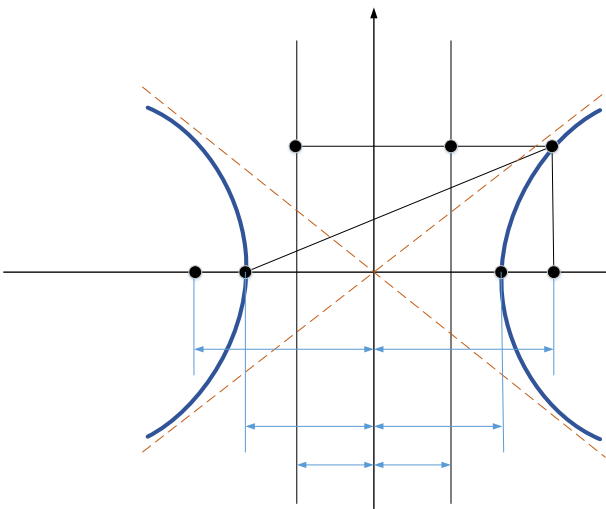

Figure 6: Graph and features of the hyperbola $\frac{x_T^2}{\alpha^2 x_A^2} - \frac{y_T^2}{(1-\alpha^2)x_A^2} = 1$

In passing, we note that though equation (58) was obtained herein as the special case ($\gamma = 1$) of equation (55), we have first obtained it by a rephrasing of the criticality condition (46) which holds for $\gamma = 1$.

Now we note that the left branch of the hyperbola lies entirely in R_r and hence it is rejected. The right branch of the hyperbola is the required Voronoi diagram, and it is bordering the escape region R_e which extends to its left. Clearly, it is an enlargement of the reachability region R_r. Likewise, we expect the escape region to be a subset of the AD Apollonius circle in Fig. 1a where $\gamma < 1$, and to be a superset of this circle in Fig. 1c where $\gamma > 1$.

Figure 7 is a sketch of the hyperbola (58) for $\alpha = 0.25$. the figure stresses that the right branch of the hyperbola is accepted as a Voronoi diagram while the left branch is rejected as such. Figure 5.3 is computer generated Voronoi diagrams for $\gamma = 1$ and α varying from 0 (the y_T-axis) to slightly less than 1 (the straight-line ray emanating from A and coinciding with the x_T-axis).

Now, we come to a novel and really important contribution of this paper, where we visualize the escape regions in the case of a fast Defender and a slow Defender. Figure 9 shows the AD-Apollonius circle for $\gamma = 0.8$ and $x_A = 4$ for which $I_1 = (0.444, 0)$, $E_1 = (36, 0)$, $O_1 = (18.22, 0)$, and $r_1 = 17.78$. Imposed on this circle is the quartic curve given by (55) which consists of two closed curves. There is one closed curve entirely outside the AD-Apollonius circle, i.e., entirely inside the Reachability region R_r and hence is rejected. The other closed curve is entirely inside the AD-Apollonius circle, i.e., the reachability region R_r and hence it is accepted as the Voronoi diagram. The escape region (safe region) is the *unshaded* area in this figure. Figure 5.5 generalizes Fig. 9 by demonstrating various accepted branches of the Voronoi diagram for $\gamma = 0.8$ and α as s parameter ranging from 0 (the AD-Apollonius circle) to a value approaching 1 from below (a closed curve collapsing to one barely encircling point A). This means that as α increases from 0 to 1, the safe or escape region expands from the exterior of the AD-Apollonius circle to almost the whole $x_T - y_T$ plane (excluding point A).

Now, we discuss the strikingly similar or dual case of a slow Defender. Figure 11 shows the AD-Apollonius circle for $\gamma = 1.25$ and $x_A = 4$ for which $I_1 = (-0.444, 0)$, $E_1 = (-36, 0)$, $O_1 = (-18.22, 0)$, $r_1 = 17.78$. Imposed on this circle is the quartic curve given by (55). Note that the whole graph in Fig. 11 is a *mirror image* of that in Fig. 9. The quartic curve again consists of two closed curves. There is one closed curve entirely inside the AD-Apollonius circle. i.e., entirely inside the Reachability region R_r and hence is rejected. The other closed curve is entirely outside the AD-Apollonius circle, i.e., entirely outside the Reachability region R_r, and hence is accepted as the Voronoi diagram. The escape region (safe region) is the *shaded* area in this figure. Figure 5.7 generalizes Fig. 11 by demonstrating various accepted branches of the Voronoi diagram for $\gamma = 1.25$ and α as a parameter ranging from 0 (the AD-Apollonius circle) to a value approaching 1 from below.

9

In passing, we discuss the situation of $\gamma = 0$ (when the Target does not move at all). In this case the TA circle collapse into a single point T and the critically condition (42) reduces to

$$(1 - \alpha^2)d^2 = 4\gamma^2 x_T x_A \qquad (64)$$

which can readily be written as

$$(x_T - (\frac{1 + \gamma^2}{1 - \gamma^2})x_A)^2 + (y_T - 0)^2 = (\frac{2\gamma x_A}{1 - \gamma^2})^2 \qquad (65)$$

an equation that can be identified as the equation of the AD Apollonius circle in the $Y_T - X_T$ coordinates. This circle serves as the Voronoi diagram for $\alpha = 0$, a fact confirming our assertion that the escape region R_e reduces to the reachability region R_r when $\alpha = 0$. Likewise, when $\gamma = 1$, imposing the condition $\alpha = 0$ on the condition (46) results in

$$x_T = 0 \qquad (66)$$

which means that the right branch of the hyperbolic Voronoi diagram (58) degenerates into the y_T−axis (the perpendicular bisector of $\overline{AD}$) and again the region R_e concides with the region R_r in this case.
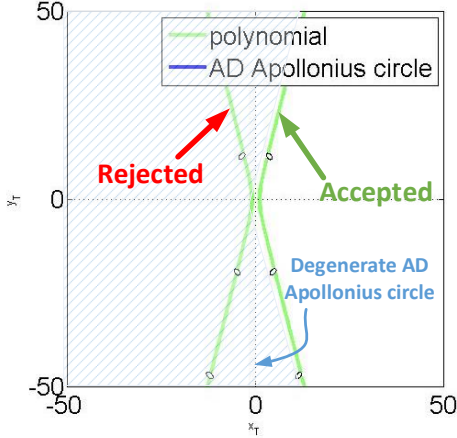

Figure 7: Generated computer output for the Voronoi diagram bordering the safe region for $x_A = 4$, $\alpha = 0.25$, $\gamma = 1$ (the safe region is the shaded area)

6. CONCLUSION AND FUTURE WORK

This paper offered a unified analytic solution of the TAD problem in which an Attacker is pursuing a Target while attempting to evade a Defender. The paper reviews and extends the work that has recently appeared in [1, 2, 3], beside making the following new contributions:

1. The paper covers all cases for the ratio γ of the Attacker's speed w.r.t. the Defender's speed. It treats the case of a slow Defender ($\gamma > 1$) for the first time, and presents this case along with the case of a fast Defender ($\gamma < 1$) discussed in [2] and the case of a similar Defender ($\gamma = 1$), discussed earlier in [1, 3].
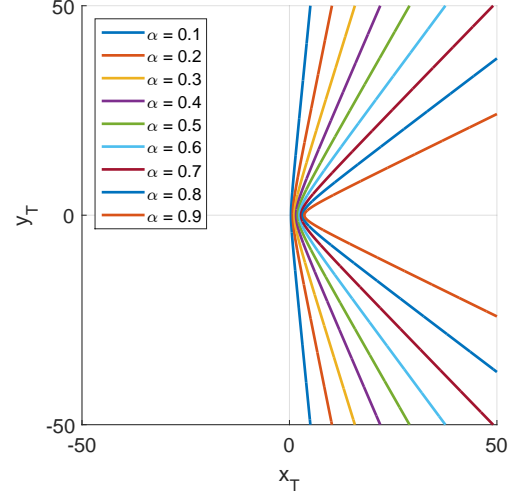

Figure 8: Various accepted branches of the voronoi diagram for $\gamma = 1$ and α as a parameter ranging from 0 to 1. These curves are computer generated from (55) and (58)

2. The paper demonstrates a striking increase in complexity when $\gamma \neq 1$ compared with the case $\gamma = 1$. It also demonstrates some sort of *duality* between the two cases of ($\gamma < 1$) and ($\gamma > 1$).

3. The paper develops novel analytic expressions for the Voronoi diagrams bordering the escape regions when ($\gamma < 1$) or ($\gamma > 1$). These expressions are more complex than the ones obtained in [3] for ($\gamma = 1$), and reduce to it as a limiting case.

4. The paper offers a tutorial exposition of the TAD problem, uses simple arguments of plane geometry to develop the necessary Apollonius circles, utilizes equalities rather than inequalities in developing Voronoi diagrams, and pays careful attention to the inadvertent inclusion of extraneous solutions so as to justify their subsequent rejection.

5. The paper supplements its analysis with extensive computations for the critical speed ratio Voronoi diagrams. The results obtained encompass all possible values of γ, and they reduce to the already available results for $\gamma = 1$.

Some possible extensions of the current work that warrant further exploration include:

1. Further analysis of the quartic equation obtained for the Voronoi diagram when $\gamma \neq 1$, with an aim to *split* it into two factors representing the rejected and accepted branches of the diagram.

2. Investigation of the sixth-degree complex polynomial equation for the optimal interception angle to get some *insight* about its six roots, and to find a better way for *selecting* the desirable root.

3. Relaxation of some of the assumptions used in this study. In particular, it is very interesting to consider the possibility of *variable* rather than constant speeds for the three agents.

4. Addition of an element of *uncertainty* to the computation. For example, we might assume that the initial positions
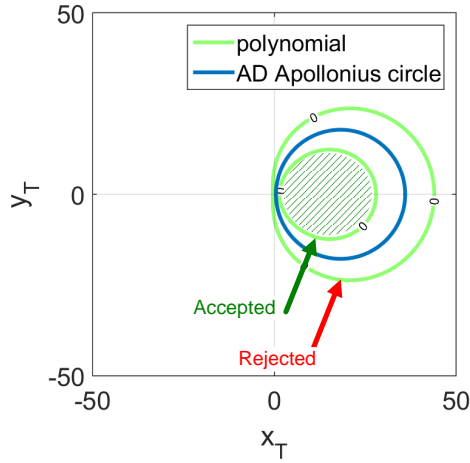
10

Figure 9: generated computer output for the Voronoi diagram bordering the safe region for $x_A = 4$, $\alpha = 0.25$, $\gamma = 0.8$ (the safe region is the unshaded area) the quartic in (54) or (55) produces two closed curves: one outside the *AD*-Apollonius circle (rejected) and the other inside the circle (accepted as the Voronoi diagram)
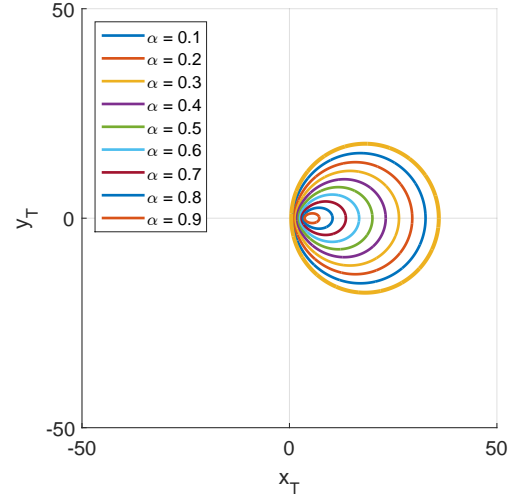

Figure 10: Various accepted branches of the voronoi diagram for $\gamma = 0.8$ and α as a parameter ranging from 0 to 1. These curves are computer generated from (55) and (58)

of the three agents are not deterministic but *stochastic* or *fuzzy*.

5. Extension of the current work to a more general situation involving several Targets, several Attackers and/or several Defenders.

References

[1] P. Meir, E. Garcia, D. W. Casbeer, Active target defense differential game, in: Proceedings of the 2014 IEEE 52nd Annual Allerton Conference on Communication, Control, and Computing, (2014), pp. 46–53.

[2] E. Garcia, D. W. Casbeer, M. Pachter, Active target defense differential game with a fast defender, arXiv preprint arXiv:1502.02747.

[3] E. Garcia, D. W. Casbeer, M. Pachter, Escape regions of the active target defense differential game, arXiv preprint arXiv:1504.07900.

[4] E. Garcia, D. W. Casbeer, K. Pham, M. Pachter, Cooperative aircraft defense from an attacking missile, in: Decision and Control (CDC), 2014 IEEE 53rd Annual Conference on, (2014), pp. 2926–2931.

[5] E. Garcia, D. W. Casbeer, K. Pham, M. Pachter, Cooperative aircraft defense from an attacking missile using proportional navigation, in: 2015 AIAA Guidance, Navigation, and Control Conference, (2015), pp. 2015–0337.

[6] E. Garcia, D. W. Casbeer, M. Pachter, Cooperative strategies for optimal aircraft defense from an attacking missile, Journal of Guidance, Control, and Dynamics ((2015)) 1–11.

[7] Y.-C. Ho, A. E. Bryson, S. Baron, Differential games and optimal pursuit-evasion strategies, in: Joint Automatic Control Conference, no. 3, (1965), pp. 37–40.

[8] R. Isaacs, Differential games III, Wiley, (1954).

[9] L. Meier, A new technique for solving pursuit-evasion differential games, in: Joint Automatic Control Conference, no. 7, 1969, pp. 514–521.

[10] M.-H. Hsueh, C.-I. Huang, L.-C. Fu, A differential game based guidance law for the interceptor missiles, in: Industrial Electronics Society, 2007. IECON 2007. 33rd Annual Conference of the IEEE, (2007), pp. 665–670.

[11] L. Yi, Y. Yan, G. Tian, J. Zhanrong, An improved terminal guidance algorithm based on differential game theory, in: Intelligent System Design and Engineering Application (ISDEA), 2010 International Conference on, Vol. 1, (2010), pp. 250–254.

[12] A. Bressan, Noncooperative differential games. a tutorial, Department of Mathematics, Penn State University.

[13] A. Perelman, T. Shima, I. Rusnak, Cooperative differential games strategies for active aircraft protection from a homing missile, Journal of Guidance, Control, and Dynamics 34 (3) ((2011)) 761–773.

[14] S. Battistini, T. Shima, Differential games missile guidance with bearings-only measurements, Aerospace and Electronic Systems, IEEE Transactions on 50 (4) ((2014)) 2906–2915.

[15] Y. Yavin, M. Pachter, Pursuit-evasion differential games, Elsevier, (2014).

[16] R. Boyell, Defending a moving target against missile or torpedo attack, Aerospace and Electronic Systems, IEEE Transactions on (4) (1976) 522–526.

[17] N. Shneydor, Comments on" defending a moving target against missile or topedo attack", IEEE Transactions on Aerospace and Electronic Systems 3 (AES-13) (1977) 321.

[18] I. Rusnak, The lady, the bandits, and the bodyguards–a two team dynamic game, in: Proceedings of the 16th World IFAC Congress, (2005).

[19] I. Rusnak, Guidance laws in defense against missile attack, in: Electrical and Electronics Engineers in Israel, 2008. IEEEI 2008. IEEE 25th Convention of, (2008), pp. 090–094.

[20] J. de Lope, D. Maravall, et al., Analysis and solution of a predator–protector–prey multi-robot system by a high-level reinforcement learning architecture and the adaptive systems theory, Robotics and Autonomous Systems 58 (12) ((2010)) 1266–1272.

[21] I. Rusnak, H. Weiss, G. Hexner, Guidance laws in target-missile-defender scenario with an aggressive defender, in: Proceedings of the 18th IFAC World Congress, Vol. 18, International Federation of Automatic Control Laxenburg, Austria, (2011), pp. 9349–9354.

[22] Z. E. Fuch, P. P. Khargonekar, Encouraging attacker retreat through defender cooperation, in: Decision and Control and European Control Conference (CDC-ECC), 2011 50th IEEE Conference on, (2011), pp. 235–242.

[23] W. Scott, N. E. Leonard, Pursuit, herding and evasion: A three-agent model of caribou predation, in: American Control Conference (ACC), 2013, (2013), pp. 2978–2983.

[24] S. Rubinsky, S. Gutman, Three-player pursuit and evasion conflict, Journal of Guidance, Control, and Dynamics 37 (1) ((2013)) 98–110.

[25] D. W. Oyler, P. T. Kabamba, A. R. Girard, Pursuit-evasion games in the presence of a line segment obstacle, in: Decision and Control (CDC), 2014 IEEE 53rd Annual Conference on, (2014), pp. 1149–1154.

[26] G. Anderson, A model for the bat versus moth pursuit-evasion problem, The Journal of the Acoustical Society of America 64 (S1) (1978) S88–S88.

[27] G. F. Miller, D. Cliff, Co-evolution of pursuit and evasion I: Biological and game-theoretic foundations, University of Sussex, School of Cognitive and Computing Sciences, (1994).

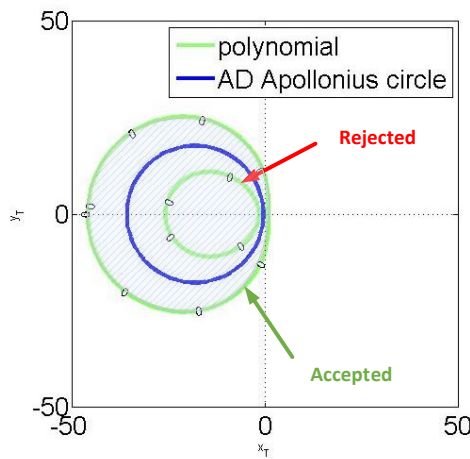[28] D. Cliff, G. F. Miller, Co-evolution of pursuit and evasion ii: Simulation

Figure 11: generated computer output for the Voronoi diagram bordering the safe region for $x_A = 4$, $\alpha = 0.25$, $\gamma = 1.25$ (the safe region is the shaded area) the quartic in (54) or (55) produces two closed curves: one inside the *AD*-Apollonius circle (rejected) and the other outside the circle (accepted as the Voronoi diagram)
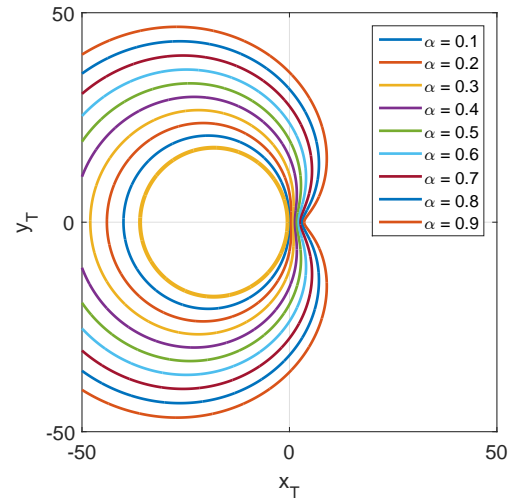

Figure 12: Various accepted branches of the voronoi diagram for $\gamma = 1.25$ and α as a parameter ranging from 0 to 1. These curves are computer generated from (55) and (58)

methods and results.

[29] A. Pekalski, A short guide to predator-prey lattice models, Computing in Science and Engineering 6 (1) ((2004)) 62–66.

[30] P. Zarchan, Tactical and strategic missile guidance, Progress in astronautics and aeronautics.

[31] P. Hagedorn, J. Breakwell, A differential game with two pursuers and one evader, Journal of Optimization Theory and Applications 18 (1) (1976) 15–29.

[32] H. Kim, Multiagent pursuit-evasion games: algorithms and experiments, (2001).

[33] Z. E. Fuchs, P. P. Khargonekar, J. Evers, Cooperative defense within a single-pursuer, two-evader pursuit evasion differential game, in: Decision and Control (CDC), 2010 49th IEEE Conference on, (2010), pp. 3091–3097.

[34] S. Pan, H. Huang, J. Ding, W. Zhang, D. M. Stipanovic, C. J. Tomlin, Pursuit, evasion and defense in the plane, in: American Control Conference (ACC), 2012, (2012), pp. 4167–4173.

[35] R. Ragesh, A. Ratnoo, D. Ghose, Analysis of evader survivability enhancement by decoy deployment, in: American Control Conference (ACC), 2014, (2014), pp. 4735–4740.

[36] A. B. Ayoub, Proving the circle of apollonius theorem, The Mathematics Teacher ((2003)) 400–401.

[37] A. B. Ayoub, On the circle of apollonius., Mathematics and Computer Education 40 (3) ((2006)) 198–204.

[38] M. B. Partensky, The circle of apollonius and its applications in introductory physics, The Physics Teacher 46 (2) ((2008)) 104–108.

[39] N. L. Fulton, U. H.-N. Huynh, Conflict management: Apollonius in airspace design, Safety science 72 ((2015)) 9–22.

[40] I. G. Gowda, D. G. Kirkpatrick, L. DER TSAI, A. Naamad, Dynamic voronoi diagrams, IEEE Transactions on Information Theory 29 (5) (1983) 724–731.

[41] F. Aurenhammer, Voronoi diagramsa survey of a fundamental geometric data structure, ACM Computing Surveys (CSUR) 23 (3) ((1991)) 345–405.

[42] W. Cheung, W. Evans, Pursuit-evasion voronoi diagrams in ell_1, in: Voronoi Diagrams in Science and Engineering, 2007. ISVD'07. 4th International Symposium on, (2007), pp. 58–65.

[43] M. L. Gavrilova, Generalized voronoi diagram: a geometry-based approach to computational intelligence, Vol. 158, Springer, (2008).

[44] I. Majdandzic, C. Trefftz, G. Wolffe, Computation of voronoi diagrams using a graphics processing unit, in: Electro/Information Technology, 2008. EIT 2008. IEEE International Conference on, (2008), pp. 437–441.

[45] E. Bakolas, P. Tsiotras, Optimal pursuit of moving targets using dynamic voronoi diagrams, in: Decision and Control (CDC), 2010 49th IEEE Conference on, (2010), pp. 7431–7436.

[46] E. Bakolas, P. Tsiotras, The zermelo–voronoi diagram: a dynamic partition problem, Automatica 46 (12) ((2010)) 2059–2067.